An investigation of internally geared screw compressor performance using a chamber modelling approach

Halil Lacevic, Ahmed Kovacevic, Matthew Read

Department of Mechanical Engineering and Aeronautics,
City, University of London,
halil.lacevic@city.ac.uk

Abstract. Gerotor machines are commonly used as oil and fuel pumps, and as hydraulic pumps and motors. They also have the potential to be used as positive displacement compressors, which is the focus of current research. The mechanism consists of an inner and outer rotor which rotate in the same direction but are each centred on offset parallel axes. The rotor profiles are specified such that multiple continuous contact points occur between them forming several separate working chambers, whose volume varies from minimum to maximum and back to minimum during a single rotation of the outer rotor. For a gas or two-phase working fluid, varying the discharge port geometry allows internal compression to occur prior to discharge. Furthermore, adding helical twist to the rotors allows the forces and torques acting on the rotors to be modified in order to minimize contact forces and power transfer between the driven and idler rotors. Previous research has investigated the operation of these internally geared screw machines via characterization of key geometrical properties and simplified analysis of the compression process. The current paper describes progress made on incorporating the geometrical analysis of these machines with the existing quasi one-dimensional chamber model within the in-house performance prediction software. This has allowed the compression process to be analysed in detail, including consideration of leakage flows and port flow losses. The influence of a range of factors including rotor profile, dimensions, built-in volume index and wrap angle have been considered through the parametric study over a range of inlet and discharge conditions.

Keywords: chamber modelling, internally geared screw machine, screw compressor

1 Introduction

Internally geared positive-displacement machines have not been extensively investigated for compressor applications, but are relatively common as liquid gerotor pumps. The gerotor pump consists of two straight-cut rotors which rotate in the same direction about non-coincident parallel axes[1] and are commonly

used in fuel and oil pumping applications and as hydraulic motors. The profiles of gerotor pump rotors are generated such that the continuous contact between the rotors is achieved. Porting in the casing then controls the period during which fluid is allowed to enter or leave the working chambers. While these ports are largely symmetrical in gerotor pumps, they can be sized to allow compression or expansion of a trapped mass of fluid to be achieved[2]. A 3D model and a cross-sectional view of a prototype internally geared screw machine are shown in Figure 1. Previous studies on the internally geared screw machine investigated different geometries and methods to generate internally geared profiles with continuous contact between them and potential advantages have been presented[3, 4].

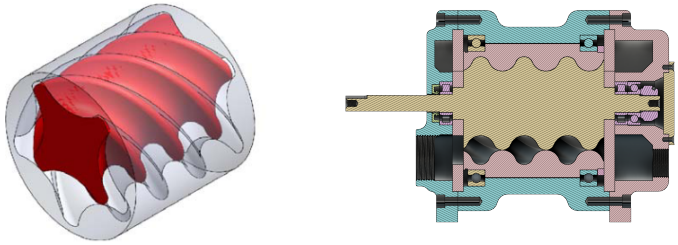

(a) Internally geared screw machine model[5]

(b) Cross-sectional view of the internally geared screw machine prototype

Fig. 1: Internally geared screw machine

Apart from understanding the geometry of the machine, an important factor determining the compressor performance is the effect of internal leakage flows. Internally geared screw machine has axial, radial, interlobe and end face leakage paths. The length of the leading and trailing edges of the volume contained between two rotors can be found by tracking the contact points throughout the working chamber for the internally geared screw machine. However, unlike the conventional machines, the internally geared machines have no 'blow-hole' leakage area as the helix on both rotors has the same orientation[3].
The objective of this study is to, for the first time, use chamber modelling approach in order to investigate thermodynamic results for different configurations of internally geared screw machines for oil injected applications for compression of air between 1 and 8 *bar*. A performance calculation and design software for rotary positive displacement machines, SCORG, which was developed at City, University of London[6] is used for thermodynamic calculations in this paper. Internally geared profile generation as well as geometry calculations were in this study implemented and integrated with the SCORG software allowing the usage of existing quasi one-dimensional chamber thermodynamic modelling feature with the internally geared screw machine geometry.

2 Thermodynamic of the Compression-Expansion Process

To perform thermodynamic calculations, SCORG software solves a nonsteady flow internal energy equation and calculation of the remaining thermodynamic and fluid properties within the machine through several cycles until the solution converges[7], as follows:

$$\omega \frac{dU}{d\Psi} = (\dot{m}h)_{in} - (\dot{m}h)_{out} + \dot{Q} - \omega p \frac{dV}{d\Psi} \tag{1}$$

$(\dot{m}h)_{in}$ represents the energy gain due to the gas inflow into the working volume by the mass inflow, while the energy loss due to the gas outflow is defined by the product of the mass outflow and its average gas enthalpy $(\dot{m}h)_{out}$. ω, Ψ represent the angular velocity and angle of rotation of the main rotor, respectively. Internal energy is presented by U and the heat transfer between the fluid and the compressor surrounding is presented by $\dot{Q}$.
The used mass continuity equation is:

$$\omega \frac{dm}{d\Psi} = \dot{m_{in}} - \dot{m_{out}} \tag{2}$$

$\dot{m_{in}}$ and $\dot{m_{out}}$ are the mass inflow and outflow rates, respectively, while each of the mass flow rates are calculated as:

$$\dot{m} = w\rho A \tag{3}$$

The instantaneous density ρ is obtained from the instantaneous mass trapped in the control volume and the size of the corresponding instantaneous volume V as $\rho = \frac{m}{V}$ and w is the fluid velocity. The equations of energy and continuity are solved to obtain $U(\Psi)$ and $m(\Psi)$. Together with $V(\Psi)$, the specific internal energy $u = U/m$ and specific volume $v = \frac{V}{m}$ are now known and temperature T as well as the pressure inside the working chamber p can be calculated for an ideal gas:

$$T = (\gamma - 1)\frac{u}{R}, \qquad p = \frac{RT}{v} \tag{4}$$

Adiabatic exponent γ, gas constant R, specific volume v and specific internal energy are predetermined. Expressing the clearance flow leakage $\dot{m}_l$ in terms of local variables (discharge coefficient μ_l, fluid velocity w_l and flow cross-sectional area A_l) at a particular position in the machine can be obtained using the following equation:

$$\dot{m}_l = \mu_l w_l \rho_l A_l \tag{5}$$

The leakage gas velocity is calculated from the differential momentum equation, accounting for the fluid-wall friction as:

$$w_l dw_l + \frac{dp}{\rho} + f\frac{w_l^2}{2}\frac{dx}{D_e} = 0 \tag{6}$$

The friction coefficient f is dependent on the local Reynolds and Mach numbers, as well as the shape of the clearance gap. Assuming constant enthalpy throttling process, the working fluid temperature will change only slightly, thus it's density may be treated as a pressure function only. The continuity equation may then be integrated between the high and low pressure sides of the gap to yield:

$$\dot{m}_l = \mu_l A_l \sqrt{\frac{p_2^2 - p_1^2}{RT_2[\zeta + 2\ln(p_2/p_1)]}} \tag{7}$$

where R is the gas constant, T_2 is the fluid temperature at high pressure side, ζ is the flow resistance and p_2, p_1 are pressures on high and low pressure side, respectively. Thermodynamic process of a compressor is described in detail by Hanjalic, Stosic[7] and model used to perform thermodynamic calculations in this paper is based on these equations. Injecting oil inside the compressor chambers has several advantages, such as cooling the compressing fluid, lubricating the meshing rotors and other clearance gaps, and preventing internal leakages, however, this interaction between the oil films and the rotors leads to a drag power loss[8]. In screw machines, oil creates drag losses through three different leakage paths: axial, interlobe, and radial. However, since the rotors co-rotate meaning their sliding velocity is very small, oil drag loss in the interlobe gap is negligible, thus is not considered in the calculation. The oil drag power P_o is calculated using the Equation 8 where $F_d^{(r)}$ and $F_d^{(a)}$ represents radial and axial drag forces respectively, while $W_{(r)}$ and $W_{(a)}$ represent the corresponding velocities related to radial and axial drag force.

$$P_o = F_d^{(r)} \cdot W_{(r)} + F_d^{(a)} \cdot W_{(a)} \tag{8}$$

Drag force is calculated based on the shear stress of oil τ_{oil} and the area on which that shear stress is applied to, A_{gap}. The drag forces $F_d^{(i)}$ $(i = r, a)$ are related only to the radial and axial gaps. The relation used to calculate the shear stress in radial and axial gaps is presented in the Equation 9 where ρ_{gap} and μ_{gap} represents density and viscosity of the fluid in the gap respectively and δ_{gap} is the actual size of the clearance gap, either radial or axial.

$$\tau_{oil} = \frac{\rho_{gap} \cdot \mu_{gap} \cdot W_{tip}}{\delta_{gap}} \tag{9}$$

Drag force, F_d, calculation for axial and radial drag force is based on the Equation 10 where A_{gap} represents the surface area of the gap calculated by gap length and depth.

$$F_d = \tau_{oil} \cdot A_{gap} \tag{10}$$

The oil drag power calculation takes into account the main rotor (inner) tip speed $W_a = W_{tip}$ in order to calculate axial shear stress and oil drag loss. Since radial drag force occurs between the inner and outer rotors providing different relative velocity between the two surfaces, radial shear stress and drag loss calculation

is function of the sliding velocity between the two rotors $W_r = W_{12}$ at the contact point. Sliding velocity equations and detailed explanation used in this research are presented by authors[9, 10]. For the purpose of this research, sliding velocity W_{12} is calculated for a contact point between the two rotors in one full rotational cycle and the root mean square (RMS) method is used in order to find generalized mean value used for radial drag force calculation.

3 Thermodynamic Analysis of Internally Geared Screw Machine

Significant work has been made in the previous research towards understanding the internally geared screw machine geometry[3, 5] which allows further studies on thermodynamic of internally geared screw machines to be performed. At this stage of research, initial thermodynamic analysis of internally geared screw machines is required for understanding the overall performance of the machine. For the initial analysis, a configuration from previous research[5], referred as *Case A* in further text, that has been proven to be efficient in terms of the power transfer between the rotors is chosen. Internally geared Case A configuration is inner rotor driven and the parameters used to produce internally geared rotor profiles are presented in Table 1 (Case A) while the profiles are generated using the pin-generation method described by authors[5, 9]. Software implementing the pin-generation method as well as the geometry calculations for internally geared rotor profiling is developed and integrated with the SCORG software allowing a convenient means of generating internally geared profiles and performing geometry calculations.

Table 1: Internally geared screw machine configuration parameters for compared cases

		Case A	Case B
Number of lobes for outer rotor	N_1	5	5
Number of lobes for inner rotor	N_2	4	4
Non-dimensional pin-center parameter	λ	1.4	1.4
Non-dimensional pin-radius parameter	σ_{bar}	0.99	0.99
Rotor length to outer profile diameter ratio	L/D	1	1
Outer rotor diameter	D	185mm	145mm
Volume index	VI	5	4
Outer rotor wrap angle	Φ_1	209°	52.25°

It should be noted that the particular profile shape parameters chosen for the current study are based on previous studies which do not consider the effects of leakage, and future work will focus on full geometrical optimisation of the internally geared machine. The aim of the current study is to demonstrate the functionality of the software that will be used for optimisation and identify aspects of the machine performance modelling that may require further attention. Thermodynamic calculations were performed for the internally geared screw machine Case A configuration and gas mass flow rate of $M_0 = 0.0951$ is obtained. Sliding velocity magnitude as well as the calculated RMS value used in oil drag loss calculation for radial gaps for the Case A configuration are shown in Figure 2.

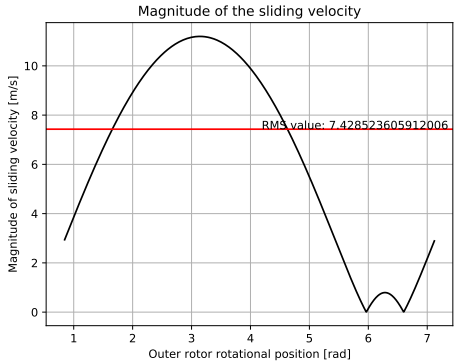

Fig. 2: Magnitude of the sliding velocity for internally geared Case A configuration showing the obtained RMS value of the sliding velocity

Performed parametric study was based on the same profile shapes as Case A (non-dimensional parameters $\lambda = 1.4$ and $\sigma_{bar} = 0.99$) and number of lobes ($N_1 = 5$, $N_2 = 4$) with different values of the outer rotor length-to-diameter ratio (L/D) and wrap angle (Φ_1). In order to compare different configurations, the same gas mass flow rate M_0 is maintained (within the accepted error of 5%) by varying the outer rotor diameter. Additionally, volume index VI has been varied for each case in order to achieve the lowest specific power. Outer rotor length to diameter ratio (L/D) varied values are $L/D = 0.25 \cdot i + 1$, $i \in \{0, 1, 2, 3, 4\}$, outer rotor wrap angle (Φ_1) varied values are $\Phi_1 = j \cdot \Phi_n$, $j \in \{0.25, 0.5, 0.75, 1, 1.25, 1.5, 1.75\}$, $\Phi_n = 209°$ and volume index varied values are $VI = 0.5 \cdot k + 2$, $k \in \{0, 1, 2, 3, 4, 5, 6\}$. Geometry calculations consisting of the geometry of the suction, discharge and fluid injection ports, chamber volume area and leakage paths with respect to the rotor position are used as the input data for the existing quasi one-dimensional chamber modelling approach. Careful study of the lines of rotor-to-rotor contact in internally geared machines allows leakage paths which connect different working chambers to be identified. The

pressure difference across these sealing lines is a key factor in determining the internal leakage to and from a chamber during the compression process. 'Blow hole' leakage path is not present in the internally geared screw machine geometry, thus it is not considered in the geometry calculations[3], however for the purposes of the initial thermodynamic calculations, geometry simplifications have been made for the interlobe and axial end-face leakage paths.
The loci of contact points between the rotors bifurcates close to the region of the minimum volume. These two branches of the contact loci connect the working chamber to the N'th and $(N-1)$'th chambers ahead and behind. In order to use the same chamber model structure as the conventional compressor, these path have been combined into a single leakage path equivalent to the interlobe leakage, which connects to the $\pm N$'th chambers. The axial end face leakage has been estimated by assuming a leakage line length of half of the exposed working chamber perimeter for the two chambers immediately ahead and behind.
Thermodynamic calculations for all the observed internally geared screw machine configurations have been performed using fixed working conditions shown in Table 2 considering an ideal gas with an adiabatic exponent of $\gamma = 1.4$, gas constant of $R_{gas} = 287\frac{J}{kgK}$ and real gas factor of $Z = 1$.

Table 2: Thermodynamic working conditions

Suction pressure [bar]	Discharge pressure [bar]	Main rotor tip speed $[m/s]$	Suction temperature $[^\circ C]$	Oil temperature $[^\circ C]$	Discharge temperature $[^\circ C]$
1	8	32	19.85	36.85	70

Based on the thermodynamic analysis, the internally geared screw machine 4/5 configuration with the outer rotor diameter of $D = 145mm$, outer rotor-to-length ratio of $L/D = 1$, outer rotor wrap angle of $\Phi_1 = 52.25^\circ$ and volume index of $VI = 4$, referred as *Case B* in further text, provides the lowest specific power, thus it is chosen for comparison with configuration obtained from the previous studies referred as Case A. Both Case A and Case B configuration parameters are shown in the Table 1 and generated rotor profiles for the Case A and Case B configurations are shown in Figure 3. Oil injection angle is 60° with respect to the main rotor rotational position for all configurations while oil injection port diameter is varied in order to achieve the fixed discharge temperature of $70^\circ C$. Thermodynamic results including relevant powers for the Case A configuration and the Case B configuration obtained from the thermodynamic analysis are shown in Table 3 and it can be noted that with variations of the port diameters, the same discharge temperature of $\approx 70^\circ C$ is achieved. It can be observed that the Case B internally geared configuration has greater volumetric efficiency and significantly lower indicated power as well as the lower oil drag power resulting in lower specific power.

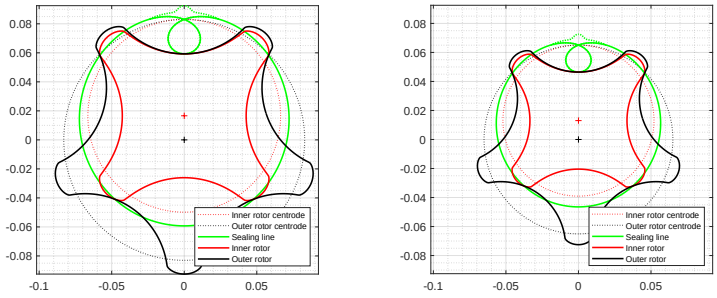

(a) Internally geared screw machine profiles for Case A (b) Internally geared screw machine profiles for Case B

Fig. 3: Internally geared screw machine profiles for compared cases

Table 3: Thermodynamic results for compared machines

Configuration	Discharge temperature [°C]	Indicated power [kW]	Oil drag power [kW]	Total power [kW]	Specific power $[\frac{\text{kW}}{(\text{m}^3/\text{min})}]$	Volumetric efficiency [%]
Case A	70.14	27.86668	0.99601	28.86269	6.013	75.72
Case B	70.06	24.65756	0.19865	24.85621	5.403	85.41

Mass flow rates as well as the oil injection port diameters and rotational speeds for both configurations are shown in Table 4. The Case B configuration has slightly lower gas mass flow rate ($\approx 4\%$) and lower oil mass flow rate resulting in lower oil-to-gas ratio. Case A configuration requests greater oil mass flow rate in order to achieve the same discharge temperature ($70°C$) as the Case B configuration, while Case B requests higher rotational speed in order to achieve the same gas mass flow rate as the Case A.

Table 4: Mass flow rates and oil injection port diameter

Configuration	Gas mass flow $[kg/s]$	Oil mass flow $[kg/s]$	Oil-to-gas ratio	Oil injection port diameter $[mm]$	Rotational speed $[RPM]$
Case A	0.0951	0.3485	3.664	5.04	4026.3
Case B	0.0912	0.2846	3.121	5.09	5137

Comparison of machine sizes for two cases showing the rotor diameters, machine lengths, overal volume of the compressor, calculated from the outer diameter and length, and the displacement volume of a single chamber are presented in Table 5. Both configurations have the same outer rotor length-to-diameter ratio $L/D = 1$, however the Case B configuration has smaller diameter $D = 145mm$ resulting in smaller machine length. The Case B configuration has lower machine

volume and lower chamber displacement volume. Additionally, volume curves for a single working chamber for both configurations are presented in the Figure 4. Based on the presented results it can be seen that Case B internally geared screw machine is smaller in overall size than the Case A configuration.

Table 5: Comparison of the Case A and Case B machine rotor diameters, lengths and volumes

Configuration	Outer/Gate rotor diameter $[mm]$	Inner/Main rotor diameter $[mm]$	Machine length $[mm]$	Machine volume $[m^3]$	Chamber volume $[m^3]$
Case A	185	151.79	185	0.004973	0.000393
Case B	145	118.97	145	0.002394	0.000262

Thermodynamic results for the Case A internally geared configuration showing the pressure as well as the mass flows in the working chamber with respect to the main rotor rotational position are shown in Figure 5 (a) and (b) respectively. Thermodynamic results for the Case B internally geared configuration showing the pressure as well as the mass flows in the working chamber with respect to the main rotor rotational position are shown in Figure 6 (a) and (b) respectively. Figures show that the leakage in the working chamber for the Case B internally geared configuration is lower than the leakage in the working chamber for the Case A configuration. Furthermore, there is significantly less oil in the machine for the Case B configuration. Pressure diagrams show that both configurations are slightly under-compressing while the peak pressure is higher for the Case B configuration.

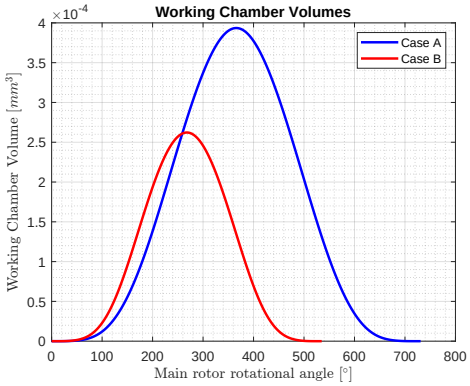

Fig. 4: Working chamber volume with respect to the main rotor rotational position for Case A and Case B configurations

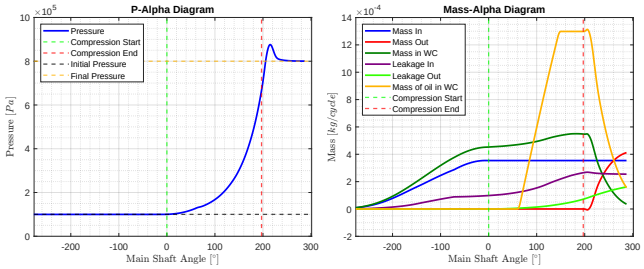

(a) P-Alpha Diagram (b) Mass-Alpha Diagram

Fig. 5: Thermodynamic results for the Case A configuration of internally geared screw machine

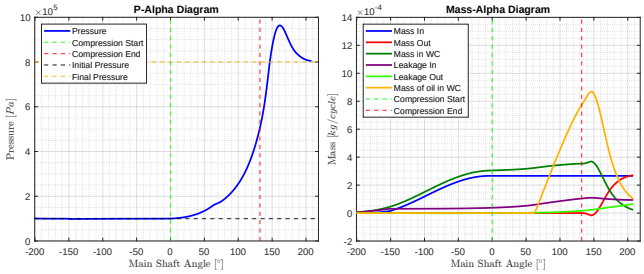

(a) P-Alpha Diagram (b) Mass-Alpha Diagram

Fig. 6: Thermodynamic results for the Case B configuration of internally geared screw machine

4 Conclusion

Thermodynamic analysis performed in this paper demonstrates capability to use one-dimensional chamber model built in SCORG to obtain performance of internally geared screw machines. The Case A configuration, obtained from the previous study, proven to be favorable in terms of the power transfer between the rotors was selected as a basis for thermodynamic analysis presented in this paper. Parametric study of the outer rotor diameter, wrap angle and length-to-diameter ratio using chamber thermodynamic model have resulted in the improved Case B geometry of the machine with the smaller rotor diameter rotating at higher speed to obtain similar mass flow rate. Volume index was varied in order to achieve the lowest specific power. The Case B configuration has lower leakage flow rate and $\approx 10.15\%$ lower specific power compared to the Case A configuration leading to more efficient compressor. Additionally, the Case B configuration reduced the outer rotor diameter and machine length by $\approx 21.6\%$ resulting in a smaller machine compared to the Case A configuration. The thermodynamic model presented in this paper can now be used for performance prediction of

internally geared screw machines. Future work should focus on experimental validation of the performance prediction and full optimization of the internally geared screw machine for a selected applications. Full comaparison of the internally geared and conventional twin screw compressors will then be performed to compare these two different configurations for selected industrial application.

Acknowledgements

Funding for this research was received from Carrier Inc., USA and PDM Analysis Ltd., UK.

References

1. Rundo M. Models for flow rate simulation in gearpumps: a review. *Energies* 2017; 10: 1261.
2. M. G. Read, I. K. Smith, and N. Stosic, "Internally geared screw machines with ported end plates," IOP Conference Series: Materials Science and Engineering, vol. 232, p. 012058, 2017. doi:10.1007/11823285_121
3. M. G. Read, I. K. Smith, and N. Stosic, "Influence of rotor geometry on tip leakage and port flow areas in Gerotor-type twin screw compressors," Proceedings of the Institution of Mechanical Engineers, Part E: Journal of Process Mechanical Engineering, vol. 236, no. 1, pp. 94–102, 2020.
4. M. Read, "Basic design procedure for an internally geared screw compressor," IOP Conference Series: Materials Science and Engineering, vol. 1180, no. 1, p. 012055, 2021.
5. M. G. Read, N. Stosic, and I. K. Smith, "The influence of rotor geometry on power transfer between rotors in gerotor-type screw compressors," Journal of Mechanical Design, vol. 142, no. 7, 2019.
6. Kovacevic A, Stosic N and Smith IK. Screw compressors: three-dimensional computational fluid dynamics and solid fluid interaction. ISBN 3-540-36302-5 Springer-Verlag Berlin Heidelberg New York, 2006
7. Hanjalic, K. and Stosic, N. (1997) 'Development and optimization of screw machines with a simulation model—PART II: Thermodynamic performance simulation and design optimization', Journal of Fluids Engineering, 119(3), pp. 664–670. doi:10.1115/1.2819296.
8. Abdan, S. et al. (2023) 'Experimental validation of the screw compressor oil drag model for various rotor profiles', Proceedings of the Institution of Mechanical Engineers, Part E: Journal of Process Mechanical Engineering, p. 095440892311635. doi:10.1177/09544089231163514.
9. D. Vecchiato, A. Demenego, J. Argyris, and F. L. Litvin, "Geometry of a cycloidal pump," Computer Methods in Applied Mechanics and Engineering, vol. 190, no. 18-19, pp. 2309–2330, 2001.
10. Ivanović, L., Josifović, D. and Ilić, A. (2013) 'Modelling of trochoidal gearing at the Gerotor Pump', Power Transmissions, pp. 553–562. doi:10.1007/978-94-007-6558-0_44.